



# Activation of Cholinergic Anti-Inflammatory Pathway Ameliorates Cerebral and Cardiac Dysfunction After Intracerebral Hemorrhage Through Autophagy

## OPEN ACCESS

### Edited by:

Richard Gordon,  
The University of Queensland,  
Australia

### Reviewed by:

Livi-Gabriel Bodea,  
The University of Queensland,  
Australia  
Nemat Khan,  
The University of Queensland,  
Australia  
Lei Huang,  
Loma Linda University, United States  
Eduardo A. Albornoz,  
The University of Queensland,  
Australia

### \*Correspondence:

Tao Yan  
taoyan@tmu.edu.cn

<sup>†</sup>These authors have contributed  
equally to this work and share  
first authorship

### Specialty section:

This article was submitted to  
Multiple Sclerosis  
and Neuroimmunology,  
a section of the journal  
Frontiers in Immunology

Received: 06 February 2022

Accepted: 23 May 2022

Published: 23 June 2022

### Citation:

Su Y, Zhang W, Zhang R, Yuan Q,  
Wu R, Liu X, Wuri J, Li R and Yan T  
(2022) Activation of Cholinergic Anti-  
Inflammatory Pathway Ameliorates  
Cerebral and Cardiac Dysfunction  
After Intracerebral Hemorrhage  
Through Autophagy.  
Front. Immunol. 13:870174.  
doi: 10.3389/fimmu.2022.870174

Yue Su<sup>†</sup>, Wei Zhang<sup>†</sup>, Ruoxi Zhang, Quan Yuan, Ruixia Wu, Xiaoxuan Liu, Jimusi Wuri,  
Ran Li and Tao Yan\*

Department of Neurology, Tianjin Medical University General Hospital, Tianjin Neurological Institute, Key Laboratory of Post-Neurotrauma, Neurorepair, and Regeneration in Central Nervous System, Ministry of Education and Tianjin City, Tianjin, China

**Background:** Intracerebral hemorrhage (ICH) is the devastating subtype of stroke with cardiovascular complications, resulting in high rates of mortality and morbidity with the release of inflammatory factors. Previous studies have demonstrated that activation of  $\alpha 7$ nAChR can reduce immune and inflammation-related diseases by triggering the cholinergic anti-inflammatory pathway (CAIP).  $\alpha 7$ nAChR mediates protection from nervous system inflammation through AMPK-mTOR-p70S6K-associated autophagy. Therefore, the purpose of this study is to explore whether the activation of  $\alpha 7$ nAChR improves cerebral and cardiac dysfunction after ICH through autophagy.

**Methods:** Male C57BL/6 mice were randomly divided into five groups **(1)**: Control + saline **(2)**, ICH+ saline **(3)**, ICH + PNU-282987 **(4)**, ICH+ PNU-282987 + MLA **(5)**, ICH + PNU-282987 + 3-MA. The neurological function was evaluated at multiple time points. Brain water content was measured at 3 days after ICH to assess the severity of brain edema. PCR, immunofluorescence staining, and Western Blot were performed at 7 days after ICH to detect inflammation and autophagy. Picro-Sirius Red staining was measured at 30 days after ICH to evaluate myocardial fibrosis, echocardiography was performed at 3 and 30 days to measure cardiac function.

**Results:** Our results indicated that the PNU-282987 reduced inflammatory factors (MCP-1, IL-1 $\beta$ , MMP-9, TNF- $\alpha$ , HMGB1, TLR2), promoted the polarization of macrophage/microglia into anti-inflammatory subtypes(CD206), repaired blood-brain barrier injury (ZO-1, Claudin-5, Occludin), alleviated acute brain edema and then recovered neurological dysfunction. Echocardiography and PSR indicated that activation of  $\alpha 7$ nAChR ameliorated cardiac dysfunction. Western Blot showed that activation of  $\alpha 7$ nAChR increased autophagy protein (LC3, Beclin) and decreased P62. It demonstrated that the activation of  $\alpha 7$ nAChR promotes autophagy and then recovers brain and heart function after ICH.

**Conclusions:** In conclusion, PNU-282987 promoted the cerebral and cardiac functional outcomes after ICH in mice through activated  $\alpha 7$ nAChR, which may be attributable to promoting autophagy and then reducing inflammatory reactions after ICH.

**Keywords:** intracerebral hemorrhage,  $\alpha 7$ nAChR, autophagy, inflammation, macrophage

## INTRODUCTION

Intracerebral hemorrhage (ICH), accounts for 10–15% of strokes (1), remains the leading cause of morbidity and mortality and is associated with severe long-term disability. Brain injury after ICH includes the consequences of primary physical trauma and enlarged hematoma, secondary brain injury (SBI) such as cerebral edema, blood-brain barrier disruption, neuronal death and inflammation may also occur (2), it is characterized by activation of microglia, induction of pro-inflammatory factors and migration of peripheral inflammatory cells into the central nervous system (CNS) (3–5). Our previous research in mice has shown that even with the lack of primary heart disease or risk factors such as hypertension, old age, or diabetes, brain injuries including subarachnoid hemorrhage (SAH), ischemic stroke, ICH, or traumatic brain injury (TBI), could cause cardiac pathological remodeling and cardiac functional deficits (6–9). Acetylcholine (ACh) is a small molecule composed of choline and acetic acid. As a neurotransmitter in the central nervous system and peripheral nervous systems, it plays a key role in maintaining brain function. As one of the two dominant classes, nicotinic ACh receptors (nAChRs) are members of the cysteine-loop family of ligand-gated ion channels (10, 11). The  $\alpha 7$  receptor is one of the nAChRs which is abundantly expressed in brain, characterized by high calcium permeability and rapid desensitization (12). It is involved in cellular processes such as survival and plasticity together with higher brain functions such as memory and learning (13). In addition,  $\alpha 7$ nAChR is expressed on a variety of cells, including glial cells, macrophages, endothelial cells, keratinocytes, dendritic cells, and lymphocytes. Other researchers have previously shown that activation of  $\alpha 7$ nAChR can alleviate multiple types of inflammatory and immune-related disorders by triggering so-called cholinergic anti-inflammatory pathways in neurological disorders (14–16). However, the underlying mechanisms have not been absolutely elucidated.

Autophagy is a lysosome-dependent pathway of cellular self-defense. Some long-lived proteins, misfolded proteins and damaged organelles are degraded and recycled through the way of autophagy (17–19). Autophagy maintains the stability of the intracellular environment and normal cellular functions. However, excessive autophagy can impair the health of cells and eventually lead to autophagic cell death under various stress conditions. Consequently, autophagy at basal level may serve as a “double-edged sword” (20). Hematoma components (for example, ferrous citrate, hemoglobin, and thrombin) have been shown to involve in ICH-induced SBI (21). Iron-induced autophagy has been reported after ICH (22). Research in experimental autoimmune encephalomyelitis (EAE) models has demonstrated that  $\alpha 7$ nAChR

can protect against neuroinflammation *via* autophagy in monocytes and microglia (23). Using an inflammatory bowel disease (IBD) model, it has been shown that  $\alpha 7$ nAChR deficiency exacerbates the severity of IBD in DSS-induced mice, while  $\alpha 7$ nAChR activation increases autophagy and suppresses proinflammatory cytokines in BMDM *via* LPS/DSS stimulation (24). It is unclear whether autophagy is involved in  $\alpha 7$ nAChR-mediated effects of intracerebral hemorrhage.

In this research, we hypothesized that activation of  $\alpha 7$ nAChR may reduce neurological and cardiac dysfunction *via* the induction of autophagy in the brain and heart following ICH. We aimed to investigate the pathogenesis of ICH and thereby provide novel insights for the development of therapeutic strategies for ICH.

## METHODS AND MATERIALS

All experiments were performed according to the guidelines and approved by the National Institutes of Health guidelines for the Animal Care and Use Committee of Tianjin Medical University General Hospital. This study follows the guidelines to promote transparency and openness. All adequate measures were taken to minimize animal pain or discomfort.

### Experimental Groups

Adult male C57BL/6J mice (20–23g, 6–8 weeks) were obtained from Vital River Laboratory Animal Technology (Beijing, China). Mice were placed in a temperature-controlled environment for a 12-hour light-dark cycle with free access to food and water. We divided mice into five groups randomly (1) control (2); ICH (3); ICH + PNU-282987 (4); ICH + PMN-282987 + (methyllycaconitine) MLA (5); ICH + PNU-282987 + 3-MA. Mice were sacrificed at the following time points for investigations: 3 days after ICH to harvest brain tissue for brain water content; 7 days after ICH to obtain heart and brain tissue for real-time polymerase chain reaction (PCR), western blot, immunofluorescence and flow cytometry; and 30 days after ICH to harvest heart for real-time PCR and Picro-Sirius Red (PSR) staining. Echocardiographic assessment of cardiac function at 7 and 30 days after intracerebral hemorrhage.

### Drug Administration

The following drugs were used in the study: PNU-282987 (an  $\alpha 7$ nAChR agonist, 1 mg/kg/day, Abcam, ab120558) (25–27), Methyllycaconitine citrate (MLA, an  $\alpha 7$ nAChR antagonist, 1 mg/kg/day, Tocris Bioscience, 1029) (28–30) and 3-MA (an autophagy inhibitor, 10 mg/kg/day, MedChemExpress, HY-19312) (23). All drugs were injected intraperitoneally. Based on

salt weight and concentration, compounds were dissolved in 0.9% saline, the injection volume is 1 ml/kg body weight. The first dose was administered 1 hour after ICH induction, followed by daily doses at 24-hour intervals. Control animals were injected with saline.

## ICH Model

We used a collagenase injection-induced intracerebral hemorrhage model. The procedure is easy to use and simulates intracerebral hemorrhage in humans (31). ICH in mice was induced by collagenase as described above. Mice were anesthetized using 5% chloral hydrate. After placing the mouse on the stereotaxic frame, drill a 1 mm hole on the right side of the skull (2.3 mm from lateral to the midline and 0.5 mm from the front of the bregma). In the collagenase induced ICH model, 0.0375 U of bacterial collagenase was dissolved in 0.5  $\mu$ l saline solution and injected at a rate into the stratum (2.3 mm left, 0.5 mm anterior, 3.5 mm deep relative to bregma), the injection speed was 0.5  $\mu$ l/min. After the injection was completed, leave the needle in place for 15 minutes to prevent backflow, then carefully removed at a speed of 1 mm/min.

## Neurological Function and Cognitive Function Tests

All functional tests were performed by an investigator who was blinded to the experimental group. The modified neurological severity score (mNSS) and foot-fault test were performed before and 1, 3, 7, 14, 21 days after the ICH to comprehensively estimate sensory, motor, reflex, and balance functions. The foot-fault test was used to evaluate the contralateral motor function deficit. Mice were photographed walking on the irregular grid for a period in a quiet environment. Contralateral limb foot faults percentage was counted. The higher score in this test, the more severe the neurological deficit.

## Brain Water Content

After 3 days of ICH, the mice were deeply anesthetized with 10% chloral hydrate. Their brains tissue was obtained and divided into three parts: the contralateral hemisphere, ipsilateral hemisphere, and cerebellum. Then, the tissue was weighed to wet weight and dried at 100°C for 24 hours to obtain dry weight. Calculate the water content in the brain using the formula: (wet weight - dry weight)/wet weight  $\times$  100%.

## Echocardiography Measurements

A researcher blinded to the experimental group performed echocardiography for non-invasive evaluation of cardiac function in mice using a Vevo2100 High-Resolution Ultrasound System in real-time (Visual Sonics Vevo 2100, Canada) with an MS-250 ultrasound scanning transducer (model C5). Anesthetized the mouse with 5% isoflurane at 0.5 L/min mixed with 100% O<sub>2</sub> and place it on a heating pad. Use 1.0-1.5% isoflurane and 0.5 l/min 100% O<sub>2</sub> to maintain sedation during surgery. Stabilized parasternal long-axis view images using m-mode imaging. Measure or calculate the following parameters: left ventricular fractional shortening (LVFS), left ventricular ejection fraction (LVEF), interventricular septum

thickness in systole (IVS; s), interventricular septum thickness in diastole (IVS; d), left ventricle interior diameter in systole (LVID; s), left ventricle interior diameter in diastole (LVID; d), left ventricular volume in systole (LV volume; s) left ventricular volume in diastole (LV volume; d). Data were calculated using software on the ultrasound system in a blinded fashion.

## Pathological and Immunofluorescence Assessments

Heart and brain tissues were fixed in 5% paraformaldehyde for 24 hours and then embedded in paraffin or OCT. Cut coronal sections of brain and heart tissue to 7  $\mu$ m. PSR staining was used to analyze the cross-sectional area of cardiomyocytes and the composition of interstitial collagen. Tissue sections were stored at -80°C and rewarmed for 20 minutes then washed with phosphate-buffered saline (PBS) for 3  $\times$  5 min. Brain and heart slides were incubated with 0.3% triton and 3% bovine serum albumin (BSA) dissolved in PBS for 90 minutes at room temperature (37°C). The following primary antibodies were used: rabbit anti-macrophage chemokine protein-1 (MCP-1, 1:200, Abcam), rabbit anti-NADPH oxidase-2 (NOX-2, Abcam, 1:250), rabbit anti-transforming growth factor- $\beta$  (TGF- $\beta$ , Santa Cruz Biotechnology, 1:250), rabbit anti-light chain 3 (LC3, Cell Signaling Technology, 1:200). Antibodies were diluted with 0.3% triton and 3% BSA. Brain sections were conjugated with anti-LC3 overnight (12-14 h) at 4°C. Heart sections were treated with anti-TGF- $\beta$ , anti-MCP-1, anti-NOX-2 and anti-LC3 overnight at 4°C. Then washed with cold PBS 3  $\times$  10 min. Incubate slides with fluorophore-conjugated secondary antibodies for 1 hour respectively at room temperature. Sections were incubated with diamidino phenylindole (DAPI, nuclear staining, Abcam). Cover the slide with a coverslip and observe under a fluorescence microscope. Immunofluorescence quantification was performed on 4 sections, and heart and brain sections were measured by immunostaining in 5 random fields, selected using a fluorescence microscope (Olympus, Japan) under a 20x objective. Data analysis was performed using Image-Pro Plus 6.0 software.

## Quantitative Real-Time PCR

After ICH 7 days, RNA was isolated from the heart and brain using TRIzol reagent (Invitrogen) and quantitated by UV spectrophotometry at 260/280 nm. Complementary DNA (cDNA) was transcribed using the Transcription First Strand cDNA Synthesis SuperMix Kit (Transgen). PCR was operated on an Opticon 2 Real-Time PCR Detection System (Bio-Rad, Hercules, USA) with SYBR Green PCR Master Mix (Roche Diagnostics, Switzerland) and the primers. Samples were analyzed in normalized and duplicated to glyceraldehyde-3-phosphate dehydrogenase (GAPDH). The expression level of mRNA was calculated as a fold change compared to the control group. The primer sequences are as follows.

Arg-1 (FWD:GAACACGGCAGTGGCTTTAAC;REV: TGCTTAGCTCTGTCTGCTTTGC);

YM-1 (FWD:CGAGGTAATGAGTGGGTTGG;REV: CACGGCACCTCCTAAATTGT)

CD206 (FWD:CAAGGAAGGTTGGCATTGT;REV: CCTTCAGTCCTTTGCAAGC);

CD86(FWD:TTGTGTGTGTTCTGGAAACGGAG;REV:AACTTAGAGGCTGTGTTGCTGGG);  
 GAPDH(FWD:GCCAAGGCTGTGGCAAGGT;REV:TCTCCAGGCGGCACGTCAGA);  
 IL-1 $\beta$ (FWD:TCCAGGATGAGGACATGAGCAC;REV:GAACGTCACACACCAGCAGGTTA);  
 MCP-1:(FWD:CTGCTACTCATTACCAGCAAG;REV:CTCTCTCTTGAGCTTGGTGACA);  
 TNF- $\alpha$ :(FWD:TACTCCCAGGTTCTCTTCAAGG;REV:GGAGGTTGACTTCTCCTGGTA);  
 MMP-9:(FWD:AAACTCTTCTAGAGACTGGGAAGGAG;REV:AGCTGATTGACTAAAGTAGCTGGA);  
 TLR2:(FWD:TTATCTTGCGCAGTTTG CAG;REV:CTCCCACCTCAGGCTCTTTG);  
 VCAM:(FWD:CTGGGAAGCTGGAACGAAGT;REV:GCCAAACACTGACCGTGAC);  
 ZO-1:(FWD:TGAACGTCCCTGACCTTTCG;REV:CTGTGGAGACTGCGTGGAAT);  
 Claudin-5:(FWD:GTTAAGGCACGGGTAGCACT;REV:TACTTCTGTGACACCGGCAC);  
 Occludin:(FWD:TGGCAAAGTGAATGGCAAGC;REV:TCATAGTGGTCAGGGTCCGT);  
 $\alpha 7$ nAChR:(FWD:GTCCTGGTCCTATGGAGGGT;REV:AGGGCTGAAATGAGCACACA);  
 HMGB1:(FWD:AGTGGCTTTTGTCCCTCATCC;REV:GGACATTTTGCCTCTCGGCT).

## Western Blot

Cell lysates with equal amounts were extracted from the heart and brain samples for Western blot analysis. Protein concentration was measured using the bicinchoninic acid method (Thermo Scientific). Samples were loaded at 12% Tris glycine gels, subjected to sodium dodecyl sulfate–polyacrylamide gel electrophoresis, and transferred onto polyvinylidene difluoride membranes (Millipore, USA). The membrane was blocked with 5% non-fat dry milk for 2 hours and incubated with primary antibody overnight at 4°C. Immunoblotting was conducted using rabbit anti-LC3 antibody (1:1000, Cell Signaling Technology, 2775S), rabbit anti-Beclin antibody (1:1000, Cell Signaling Technology, 3495S), rabbit anti-p62/SQSTM1 antibody (1:1000, Cell Signaling Technology, 5114S), rat anti- $\alpha 7$ nAChR (1:200 Santa Cruz Biotechnology, sc-58607), mouse anti-GAPDH antibody (1:1000, Nakasugi Jinqiao). The membranes were then incubated with species-appropriate secondary antibodies for 1 hour at room temperature. The protein bands were visualized with a Bio-Rad Gel Imager.

## Flow Cytometry

The mice were sacrificed 7 days after the intracerebral hemorrhage and brain tissue was collected to prepare a single cell suspension. In brief, for all animals, the brains were removed, minced with scissors, incubated with collagenase D4 (Sigma-Aldrich, 1 mg/ml) and Dispase (Roche, 1 mg/ml) and digested at 37°C for 60 minutes. The homogenate was passed through a 70 $\mu$ m filter and the filtrate was centrifuged for 3 min at 2000 rpm. The centrifuged cells were resuspended in 30% Percoll and centrifuged for 10 min at 700  $\times$  g. The particles were washed with cold PBS for 10 minutes at

2000 rpm. Incubate the single cell suspension with the following fluorescently labeled antibodies: CD11b-FITC, CD45-Percp, F4/80-APC, CD206-PE/cy7, CD86-PE and Ly6G-APC/cy7, (BioLegend, San Diego, USA). The data of flow cytometry were acquired on a FACS Aria™ Flow cytometer (BD Biosciences, San Jose, USA) and analyzed with FlowJo software.

## Statistical Analysis

Statistics were analyzed by Graphpad Prism. Statistical analysis was conducted by unpaired 2-tailed Student t-test for comparison of two groups, one-way analysis of variance (Tukey) was used for analysis among the five groups and repeated measure analysis of variance was used to study the difference in foot-fault functional and mNSS tests. All values are expressed as mean  $\pm$  standard error, p values < 0.05 are considered statistically significant.

## RESULTS

### Activating $\alpha 7$ nAChR Decreased Brain Water Content 3 Days After ICH

To determine whether treatment with the  $\alpha 7$ nAChR agonist PNU-282987 reduces brain water content during the acute stage of ICH, brain water content was evaluated at 3 days after surgery. **Figure 1A** shows that PNU-282987 remarkably decreased water content in the ipsilateral cerebral hemisphere compared to ICH + saline group. However, MLA reversed this effect entirely. There is no significant difference between the contralateral hemisphere and the cerebellum.

### Activating $\alpha 7$ nAChR Improved Neurological Function in ICH Mice

A series of neurological and cognitive tests were performed to test the effects of PNU-282987 on neurological deficits. The foot-fault test and the mNSS were performed after ICH. The data showed that treatment with PNU-282987 reduce neurological deficits in the ICH + PNU-282987 treatment group compared to the ICH + saline group, while this treatment effect was reversed by the administration of MLA (**Figures 1B, C**).

### Activating $\alpha 7$ nAChR Prevented ICH-Induced Cardiac Dysfunction

Echocardiography was employed to test whether the cholinergic anti-inflammatory pathway ameliorated ICH-induced cardiac dysfunction. Data in **Figures 2A, B** presents typical echocardiographic data at 7 and 30 days after ICH. These data revealed that ICH induced acute (7 days) and chronic (30 days) cardiac dysfunction in mice illustrated by reduced LVEF, LVFS and IVS (d, s) compared to control group. PNU-282987 treatment remarkably improved systolic function by increasing LVEF, LVFS and IVS (d, s) at 7 and 30 days after ICH. However, MLA could reverse this effect at 30 days after ICH (**Figure 2C**). It also exhibits significant increases in LVID (d, s) and LV volume (d,s) in ICH mice at 7 and 30 days after ICH compared with controls. The treatment of PNU-282987 decreases LVID and LV volume at 7 days

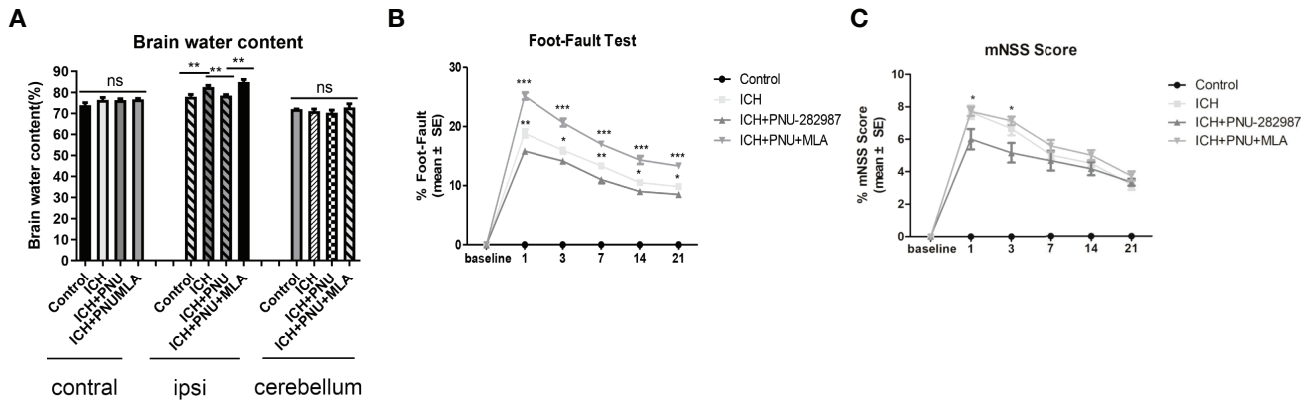


**FIGURE 1** | Activating  $\alpha 7$ nAChR decreased brain water content 3 days after ICH and improves neurological function in ICH mice. **(A)** PNU-282987 significantly reduces water content in the brain in the ipsilateral hemisphere. **(B)** Activating  $\alpha 7$ nAChR decreases foot-fault test scores in ICH mice. **(C)** Activating  $\alpha 7$ nAChR decreases mNSS scores in ICH mice.  $n = 5$ /group, the results are expressed as mean  $\pm$  SE, \* $p < 0.05$ , \*\* $p < 0.01$ , \*\*\* $p < 0.0001$ , ns means  $p > 0.05$ .

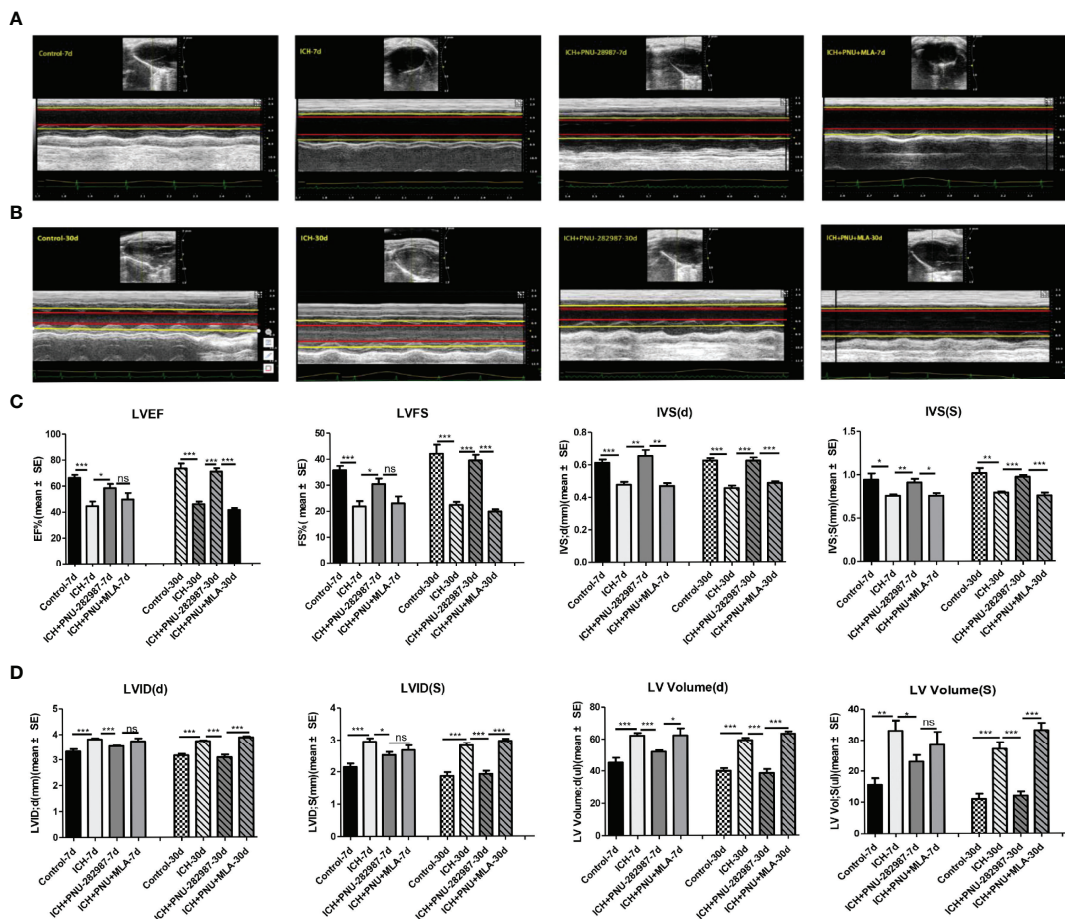


**FIGURE 2** | Activating  $\alpha 7$ nAChR prevented ICH-induced cardiac dysfunction. **(A)** Representative echocardiography results at 7 days from control, ICH, ICH+PNU-282987, ICH+PNU-282987+MLA. **(B)** Representative echocardiography results at 30 days from control, ICH, ICH+PNU-282987, ICH+PNU-282987+MLA. **(C)** LVEF, LVFS dimension at 7 days and 30 days after ICH, IVS dimension at the end of diastole and systole. **(D)** LV volume, LVID dimension at the end of diastole and systole.  $n = 6$  per group for echocardiography. Data are presented as mean  $\pm$  SE; \* $p < 0.05$ ; \*\* $p < 0.01$ ; \*\*\* $p < 0.0001$ ; ns means  $p > 0.05$ .

and 30 days, whereas MLA reversed this effect (Figure 2D). Our data suggest that ICH may lead to significant disturbances in cardiac function in both acute and chronic phases, PNU-282987 significantly attenuates myocardial dysfunction induced by ICH.

### Activating $\alpha 7$ nAChR Significantly Decreased Cardiac Fibrosis and Cardiac Hypertrophy in the Chronic Phase of ICH

In our previous studies, we discovered that ICH led to cardiac fibrosis and myocyte hypertrophy in the chronic phase of ICH. To observe the effect of  $\alpha 7$ nAChR on the heart, we detected myocardial fibrosis and cardiomyocytes using PSR 30 days after ICH. Cardiac hypertrophy was evaluated as heart weight to body weight ratio (mg/10 g). Figures 3A–D shows that ICH induced myocardial hypertrophy and fibrosis compared to control. PNU-282987 decreases cardiac hypertrophy and fibrosis compared to ICH mice. However, MLA reverses this effect. TGF- $\beta$  has been proven to play a vital role in mediating cardiac fibrosis (32). Matrix metalloproteinase-9 (MMP-9) is used as a marker for changes in the heart associated with inflammation and fibrosis (33, 34). The PCR data of TGF- $\beta$  and MMP-9 indicates that ICH significantly increases the level of TGF- $\beta$  and MMP-9 expression in the heart compared to control mice in the chronic phase of ICH. PNU-282987 significantly decreased the level of TGF- $\beta$  and MMP-9 expression compared to ICH mice, contrary to MLA's effect (Figures 3E, F). Therefore, it is concluded that activating  $\alpha 7$ nAChR significantly decreased cardiac fibrosis and cardiac hypertrophy during the chronic phase of ICH.

### Activating $\alpha 7$ nAChR Induced Autophagy in the Brain and Heart of ICH Mice

Previous studies have shown that autophagy plays a controversial role in ICH by regulating the production of inflammatory cytokines (35). Therefore, we questioned whether the protective

effect of  $\alpha 7$ nAChR activation on ICH was related to enhanced autophagy. Firstly, we used immunoblotting to test the effect of activated  $\alpha 7$ nAChR on the autophagy-related protein in the brain and heart of ICH mice. We found that activated  $\alpha 7$ nAChR by PNU-282987 significantly increased the expression level of LC3-II/I ratio and the Beclin, while reduced the expression of p62/SQSTM1 in the brain and heart after ICH. (Figures 4A–H). Secondly, we conducted further immunofluorescence staining of LC3 in the heart and brain. We found that ICH mice exhibited higher expression level of LC3 in the brain and heart compared to controls. PNU-282987 treatment could further increase the expression of LC3, while MLA blocked these effects (Figures 5A–D). Collectively, these data suggest that  $\alpha 7$ nAChR activation promotes autophagy in the brain and heart after ICH.

### The Expression of $\alpha 7$ nAChR Was Decreased in Brain and Heart After ICH

PCR and Western blotting were used to measure the expression of  $\alpha 7$ nAChR for 7 days after ICH. The data showed that protein expression of  $\alpha 7$ nAChR after ICH was decreased compared to control mice (Figures 6A–C), as well as the mRNA expression of  $\alpha 7$ nAChR (Figures 6D, E). These results demonstrate that PNU-282987 increases the expression of  $\alpha 7$ nAChR in the brain and heart of mice after ICH.

### Activating $\alpha 7$ nAChR Mediated Neuroprotection in ICH by Regulating Microglia/Macrophage Polarization Toward to an Anti-Inflammatory Phenotype

Macrophage/microglia can polarize into two phenotypes: anti-inflammatory and pro-inflammatory, producing anti- or pro-inflammatory chemokines and cytokines (36, 37). Analyse of whether activating  $\alpha 7$ nAChR alters microglia/macrophage

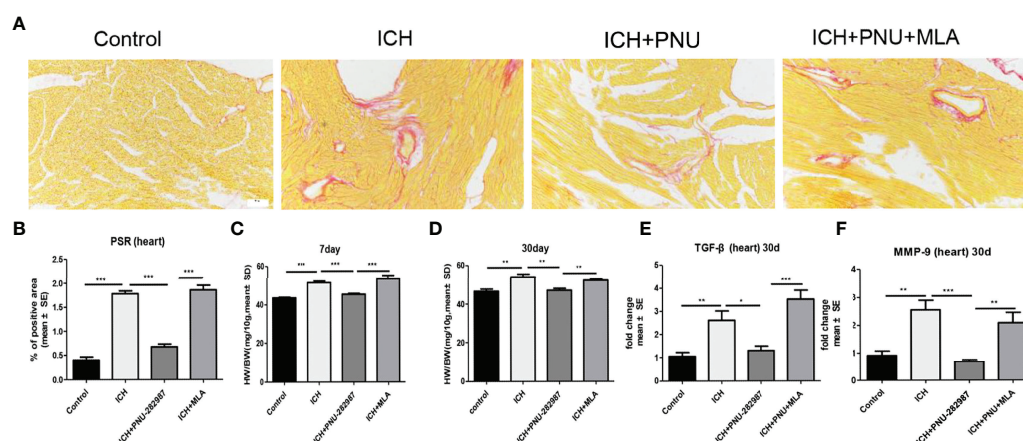


**FIGURE 3** | Activating  $\alpha 7$ nAChR significantly decreased cardiac fibrosis and cardiac hypertrophy in the chronic phase of intracerebral hemorrhage. (A) Representative results for PSR immunostaining in heart tissue at 30 days. (B) Quantification of interstitial fibrosis (Picro Sirius Red).  $n = 6$  per group. (C) The result of heart weight at 7 days. (D) The result of heart weight at 30 days. (E) The PCR results showed that treatment with PNU-282987 significantly reduced the gene expression of the ICH-caused profibrotic factor TGF- $\beta$  compared with ICH mice at 30 days. (F) PNU-282987 significantly reduced the gene expression of the ICH-caused profibrotic factor MMP-9 compared with ICH mice at 30 days.  $n = 6$  per group. Data are presented as mean  $\pm$  SE; \* $p < 0.05$ ; \*\* $p < 0.01$ ; \*\*\* $p < 0.0001$ .

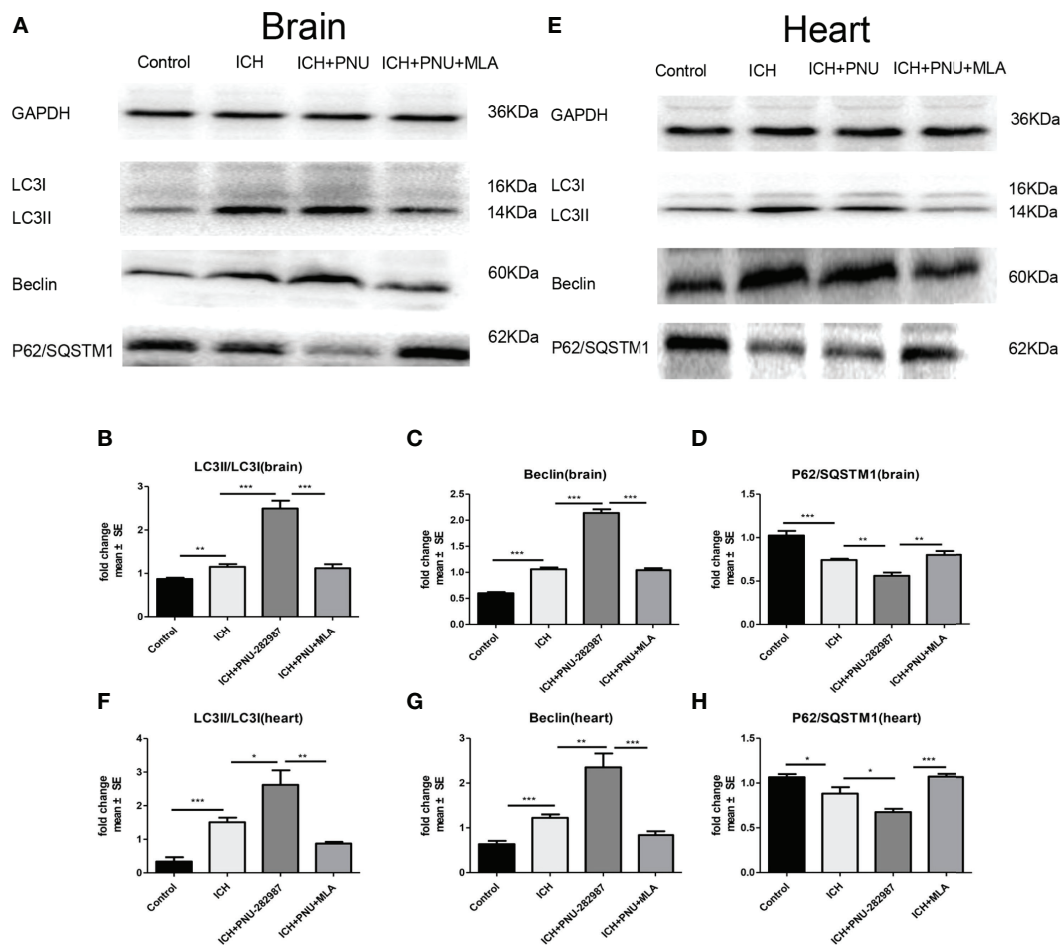


**FIGURE 4** | Activating  $\alpha 7$ nAChR induced autophagy in the brain and heart of ICH mice. **(A)** Representative protein expression levels of LC3, Beclin, p62/SQSTM1 in brain evaluated by western blot. **(B)** Quantification of western blot data of LC3 in brain. **(C)** Quantification of western blot data of Beclin in brain. **(D)** Quantification of western blot data of p62/SQSTM1 in brain. **(E)** Representative protein expression levels of LC3, Beclin, p62/SQSTM1 in heart, as measured by western blot. **(F)** Quantification of western blot data of LC3 in heart. **(G)** Quantification of western blot data of Beclin in heart. **(H)** Quantification of western blot data of p62/SQSTM1 in heart.  $n = 6$  per group. Data are presented as mean  $\pm$  SE; \* $p < 0.05$ ; \*\* $p < 0.01$ ; \*\*\* $p < 0.0001$ .

polarization, we performed flow cytometry to measure the expression of CD206 and CD86 in the brain for 7 days. We quantified the expression of pro-inflammatory markers (CD86) and anti-inflammatory markers (CD206, YM-1 and Arg-1) in brain and heart for 7 days using real-time PCR to confirm flow cytometry results. The data showed that the expression of anti-inflammatory macrophages was decreased in ICH mice compared to the control mice. PNU-282987 treatment increased anti-inflammatory macrophages expression. However, this effect was completely reversed by co-administration of MLA. The expression of pro-inflammatory macrophages was increased in ICH mice compared to the control mice. PNU-282987 treatment decreased pro-inflammatory macrophages expression. Again, the effect was completely reversed by MLA (Figures 7A–C, 8A–H).

## $\alpha 7$ nAChR Expression in Endothelial Cells Promoted Angiogenesis and Alleviated the Functional Dysfunction of the Blood–Brain Barrier After ICH

$\alpha 7$ nAChR is broadly expressed in the central and peripheral nervous systems and also in non-neuronal tissues such as endothelial cells. Activation of endothelial cells is characterized by increased expression of adhesion molecules on the cell surface (38). VCAM plays an important role in this process. In our experiment, we observed that PNU-282987 significantly increased VCAM mRNA expression (Figure 9A). Furthermore, the mRNA expression of ZO-1, Claudin-5, Occludin was increased by PNU-282987. However, the effects were completely reversed by MLA (Figures 9B–D). These data showed that activated  $\alpha 7$ nAChR

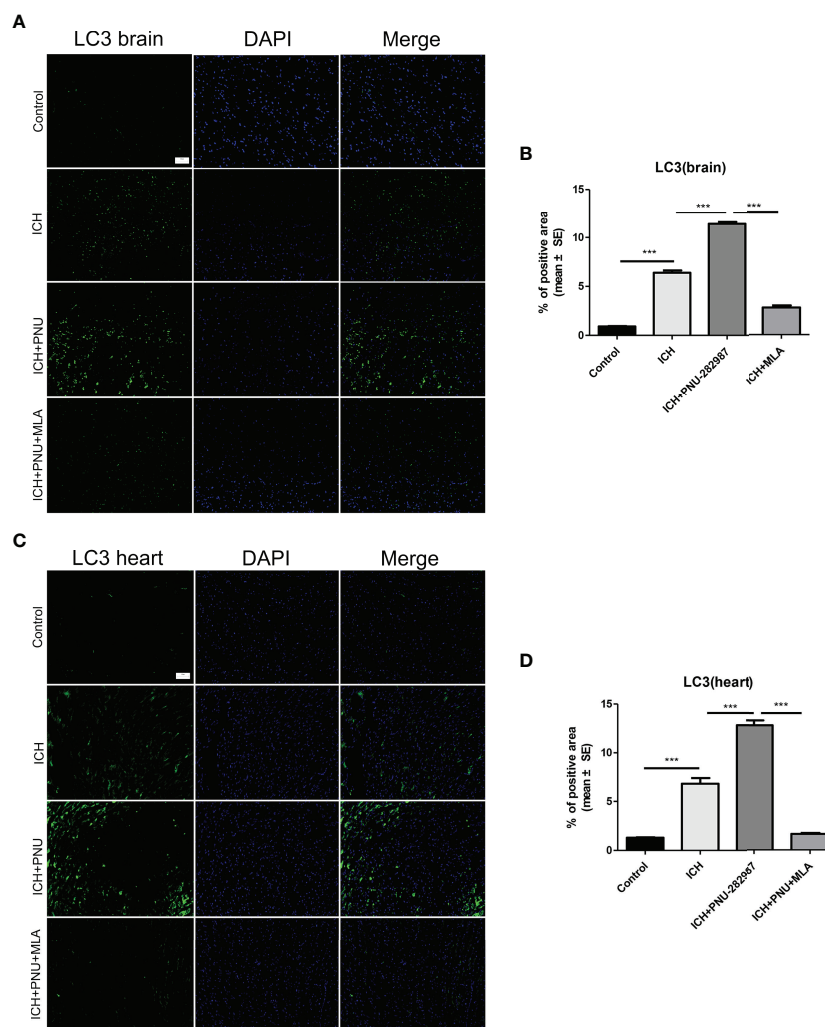


**FIGURE 5** | Activating  $\alpha 7$ nAChR induced autophagy in the brain and heart of ICH mice. **(A)** Immunofluorescence staining of LC3 from brain tissue of control, ICH, ICH+PNU-282987 and ICH+PNU-282987+MLA (scale bar, 100  $\mu$ m). **(B)** The quantitation of LC3 in brain. **(C)** Immunofluorescence staining of LC3 from heart tissue of control, ICH, ICH+PNU-282987 and ICH+PNU-282987+MLA (scale bar, 100  $\mu$ m). **(D)** The quantitation of LC3 in heart.  $n = 6$  per group. Data are presented as mean  $\pm$  SE; \*\*\* $P < 0.0001$ .

significantly induced endothelial cell activation, promoted angiogenesis and restored the function of complex blood brain barrier.

### Activating $\alpha 7$ nAChR Decreased ICH-Caused Oxidative Stress and Inflammatory Responses in the Brain and Heart

In our previous studies, it was confirmed that ICH induced cardiac inflammation (9). The mRNA expression of inflammatory factor (IL-1 $\beta$ , TNF- $\alpha$ , MCP-1, HMGB1, MMP-9 and TLR2) were measured by PCR in brain (Figures 10A–F) and heart (Figures 10G–L) tissue harvested at 7 days after ICH. To corroborate the PCR findings, we used immunofluorescence staining to measure NOX-2, MCP-1 and TGF- $\beta$  in heart tissue

(Figures 11A–F). The results showed that the inflammatory factor increased in ICH mice compared to control. PNU-282987 treatment decreased inflammatory factor expression. However, this effect was completely reversed by MLA and 3-MA. We also performed flow cytometry to measure the expression of neutrophils (CD45+ CD11b+ Ly6G+) and macrophages (CD45+ CD11b+ F4/80+). As demonstrated in Figures 7A, D–E, macrophages and neutrophils expression was significantly increased in ICH mice compared to control. Furthermore, macrophages and neutrophils were significantly reduced in the brains of PNU-282987-treated ICH mice compared with saline-treated ICH mice. However, MLA blocked these effects. The results suggest that activation  $\alpha 7$ nAChR reduced inflammatory cells infiltration into the brain after ICH.

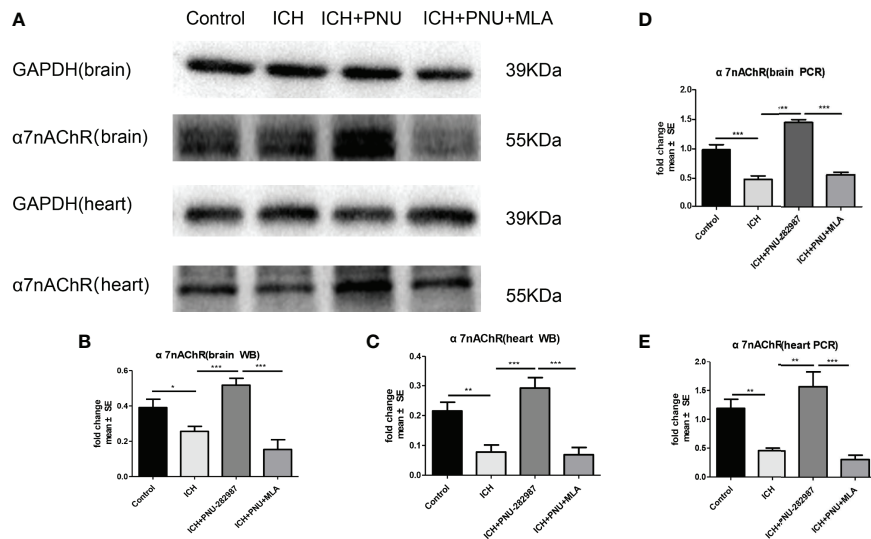


**FIGURE 6** | The expression of  $\alpha 7$ nAChR was reduced in brain and heart After ICH. **(A)** Representative protein expression levels of  $\alpha 7$ nAChR in brain and heart, the expression of protein  $\alpha 7$ nAChR remarkably reduced at 7 days after ICH, while PNU-282987 promoted their expression. **(B)** Quantification of western blot data in brain. **(C)** Quantification of western blot data in heart. **(D)** ICH for 7 days significantly decreased mRNA expression of  $\alpha 7$ nAChR in brain, PNU-282987 promoted their expression. **(E)** ICH for 7 days significantly decreased mRNA expression of  $\alpha 7$ nAChR in heart, PNU-282987 promoted their expression.  $n = 6$  per group. Data are presented as mean  $\pm$  SE; \* $p < 0.05$ ; \*\* $p < 0.01$ ; \*\*\* $p < 0.0001$ .

## DISCUSSION

We have two main conclusions from this study. First, we demonstrate that  $\alpha 7$ nAChR activation protected against ICH injury through improving neurological and cardiac dysfunction. Second, our data provided direct evidence that autophagy is causally linked to  $\alpha 7$ nAChR activation and helped to ameliorate injury. It is widely believed that the  $\alpha 7$ nAChR is involved in a systemic anti-inflammatory mechanism called the cholinergic anti-inflammatory pathway (CAIP) (39). The CAIP has recently been described as a neuroimmunomodulatory pathway whose activation may be effective in reducing the release of pro-inflammatory cytokines and suppressing inflammatory response (40, 41). The cholinergic anti-inflammatory pathway acted primarily role through stimulation of the vagus nerve in an  $\alpha 7$ nAChR-dependent manner. In macrophages,  $\alpha 7$ nAChR activation inhibited pro-inflammatory transformation and promoted anti-inflammatory polarization, thereby regulating the inflammatory response (42).

It has been demonstrated previously that activating  $\alpha 7$ nAChR played a protective effect in a variety of cardiovascular and cerebrovascular diseases, including TBI, ischemic stroke, ICH, SAH, hypertension and myocardial ischemia (43–45). In our study, The experiment result showed that PNU-292987 administered 1 h after surgery could reduce the brain edema in the ipsilateral hemisphere 3 days after ICH, This finding coincides with Krafft et al. study, which indicated that intraperitoneal injection of PNU-282987 at a dose of 12mg/kg after ICH induction 1h could prevent to the increase in basal ganglia water

content in male CD-1 mice at 3 days (15). While Hijioka et al. showed that PNU-282987 had no significant effect on the degree of hematoma and the formation of brain edema. The discrepancy may be due to different animal models, drug doses and times of drug administration (16). Whether PNU-282987 contributes to relieve the severity of brain edema warrants further studies. A study using a permanent middle cerebral artery occlusion model demonstrated that the neuroprotective effects of activating  $\alpha 7$ nAChR on the anti-oxidative stress, reduction of pro-inflammatory and NF- $\kappa$ B activity in macrophages/microglia (46). Furthermore, the  $\alpha 7$ nAChR agonist PHA-543613 attenuated neuroinflammation in rodents after experimental intracerebral hemorrhage by activating the JAK2-STAT3 signaling pathway (47). Other studies have shown that electroacupuncture stimulation induced significant neuroprotection in neurons after transient ischemic brain injury by modulating  $\alpha 7$ nAChR to inhibit the inflammatory response associated with NLRP3 inflammation, reduce apoptosis, and modulate the balance between anti- and pro-inflammatory factors (48).

In addition to cardiovascular and cerebrovascular diseases,  $\alpha 7$ nAChR also played a significant role in other systemic diseases. For instance, it has been demonstrated that the hepatic vagus nerve played a key role in regulating the inflammatory response of Kupffer cells *via* the  $\alpha 7$ nAChR pathway and ultimately inhibited the progression of nonalcoholic steatohepatitis at an early stage (49). Peng Teng demonstrated that stimulation of  $\alpha 7$ nAChR by nicotine attenuated monosodium iodoacetate-induced

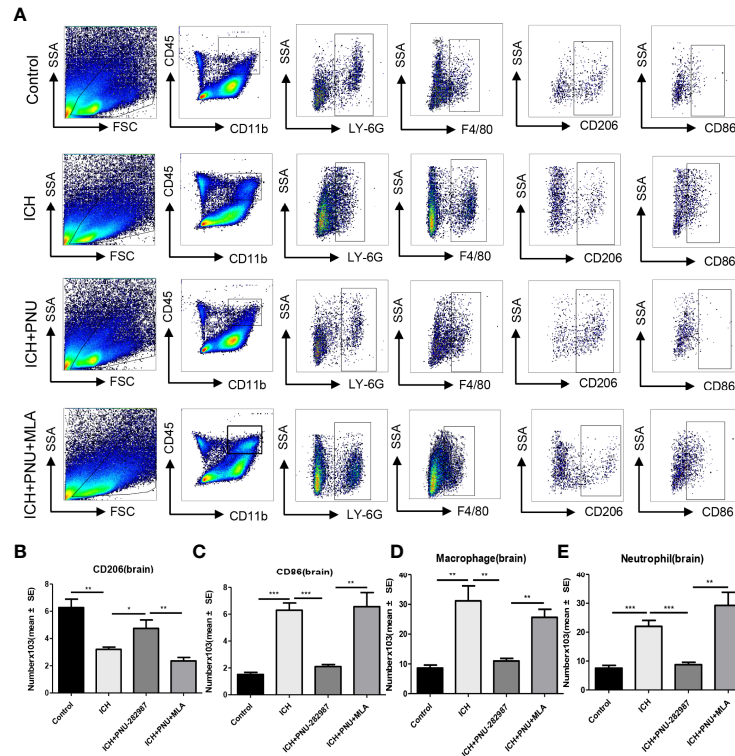


**FIGURE 7** | Activating  $\alpha 7$ nAChR mediated neuroprotection in ICH by regulating microglia/macrophage polarization toward an anti-inflammatory phenotype. **(A)** Typical flow cytometric graph showing the gating strategy for CD45+CD11b+F4/80+ macrophages, CD45+CD11b+Ly6G+neutrophils, CD206+ anti-inflammatory macrophages and CD86+ pro-inflammatory macrophages populations in brain. **(B)** Quantitative data of anti-inflammatory macrophages expression in brain at 7 days after ICH. **(C)** Quantitative data of pro-inflammatory macrophages expression in brain at 7 days after ICH. **(D)** Quantitative data of macrophages expression in brain at 7 days after ICH. **(E)** Quantitative data of neutrophils expression in brain at 7 days after ICH. Data are presented as mean  $\pm$  SE; \* $p < 0.05$ ; \*\* $p < 0.01$ ; \*\*\* $p < 0.0001$ .

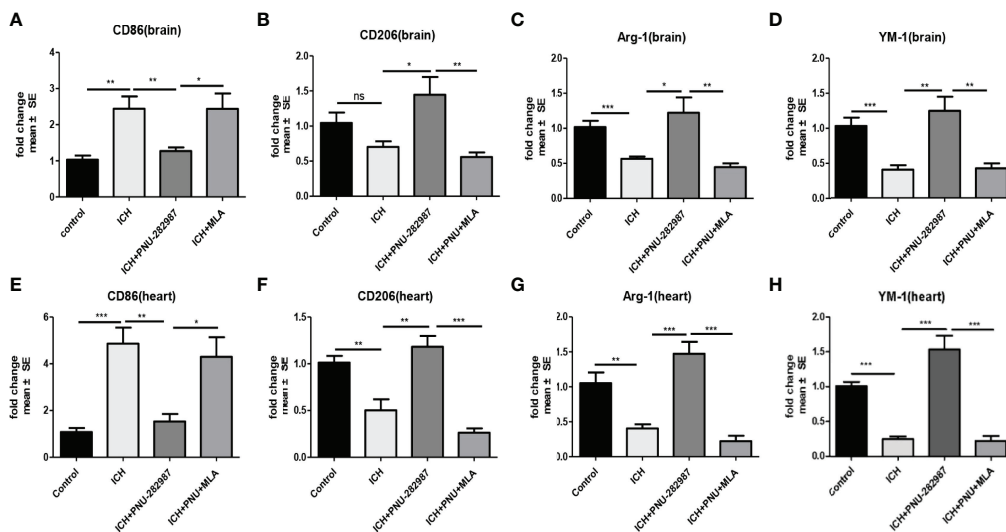


**FIGURE 8** | The results of PCR demonstrated that PNU-282987 drastically decreased the phenotype of pro-inflammatory macrophages [CD86 **(A)**] and increased anti-inflammatory macrophages [CD206 **(B)**, Arg-1 **(C)**, YM-1 **(D)**] in brain. PCR results indicated that PNU-282987 significantly reduced the pro-inflammatory macrophages [CD86 **(E)**] and increased the phenotype of anti-inflammatory macrophages [CD206 **(F)**, Arg-1 **(G)**, YM-1 **(H)**] in heart.  $n = 6$  per group for echocardiography. Data are presented as mean  $\pm$  SE; \* $p < 0.05$ ; \*\* $p < 0.01$ ; \*\*\* $p < 0.0001$ ; ns means  $p > 0.05$ .

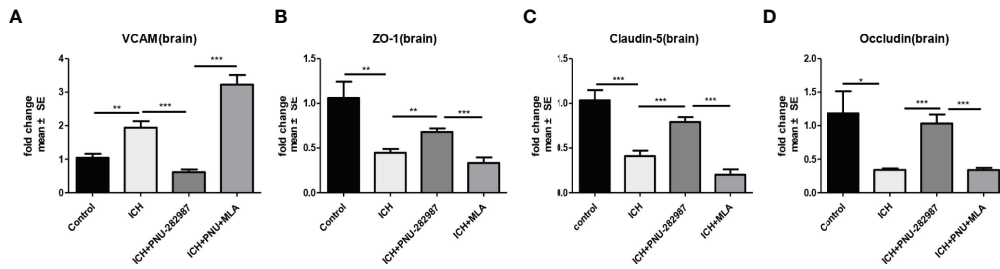


**FIGURE 9** |  $\alpha 7$ nAChR expression in endothelial cells promoted angiogenesis and alleviated the functional dysfunction of the blood–brain barrier after ICH. **(A)** PCR results indicated that PNU-282987 remarkably decreased the expression of VCAM. **(B)** The results of PCR demonstrated that PNU-282987 drastically increased the expression of ZO-1. **(C)** The results of PCR demonstrated that PNU-282987 drastically increased the expression of Claudin-5. **(D)** The results of PCR demonstrated that PNU-282987 drastically increased the expression of Occludin. n = 6 per group for echocardiography. Data are presented as mean  $\pm$  SE; \*p < 0.05; \*\*P < 0.01; \*\*\*P < 0.0001.

cartilage degradation and osteoarthritis pain, this protective effect of nicotine is associated with the inhibition of MMP-9 overexpression *via* the PI3K/Akt/NF- $\kappa$ B signaling pathway (50).

The various underlying mechanism of the cholinergic anti-inflammatory pathway after stroke has been extensively studied by several groups (51). A study showed that activation of  $\alpha 7$ nAChR and subsequent cholinergic anti-inflammatory

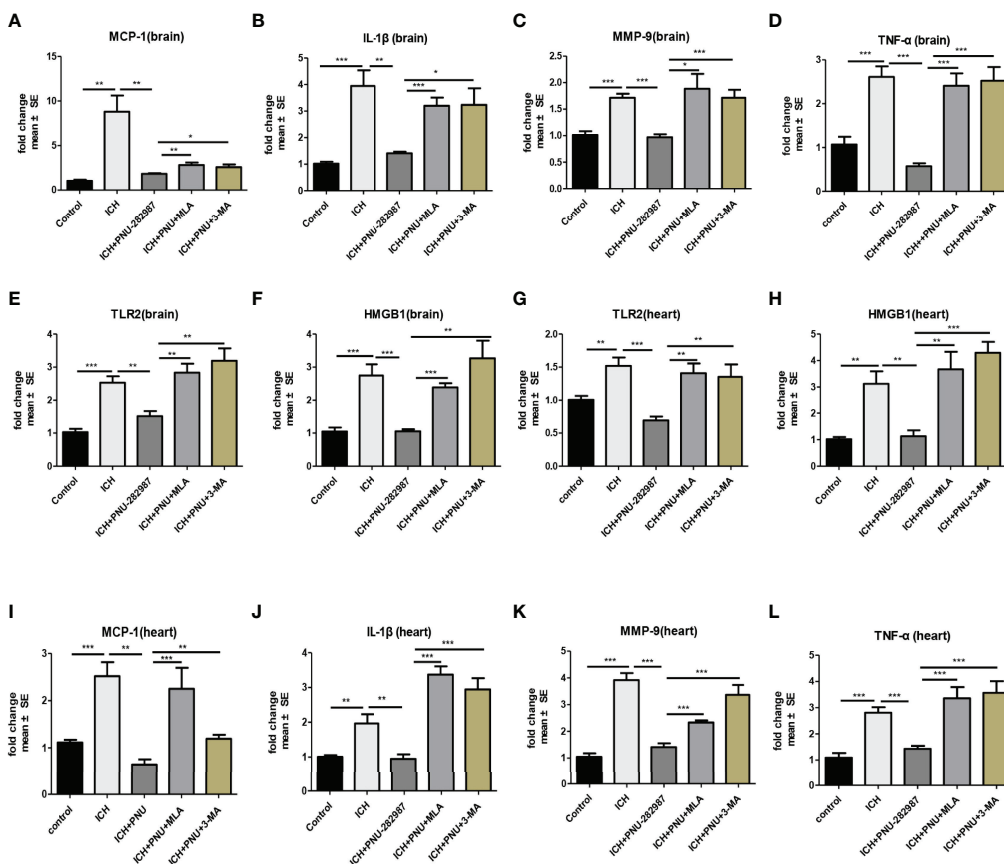


**FIGURE 10** | Activating  $\alpha 7$ nAChR decreased ICH-caused oxidative stress and inflammatory responses in the brain and heart. **(A–F)** PCR results indicated that PNU-282987 remarkably decreased ICH-induced inflammatory factor expression as MCP-1, IL- $\beta$ , MMP-9, TNF- $\alpha$ , TLR2 and HMGB1 compared to control mice in brain at 7 days after ICH. **(G–L)** PCR results indicated that PNU-282987 significantly reduced gene expression of ICH-induced inflammatory factor as TLR2, HMGB1, MCP-1, IL- $\beta$ , MMP-9 and TNF- $\alpha$  compared to control mice in heart at 7 days after ICH. n = 6 per group for echocardiography. Data are presented as mean  $\pm$  SE; \*p < 0.05; \*\*P < 0.01; \*\*\*P < 0.0001.

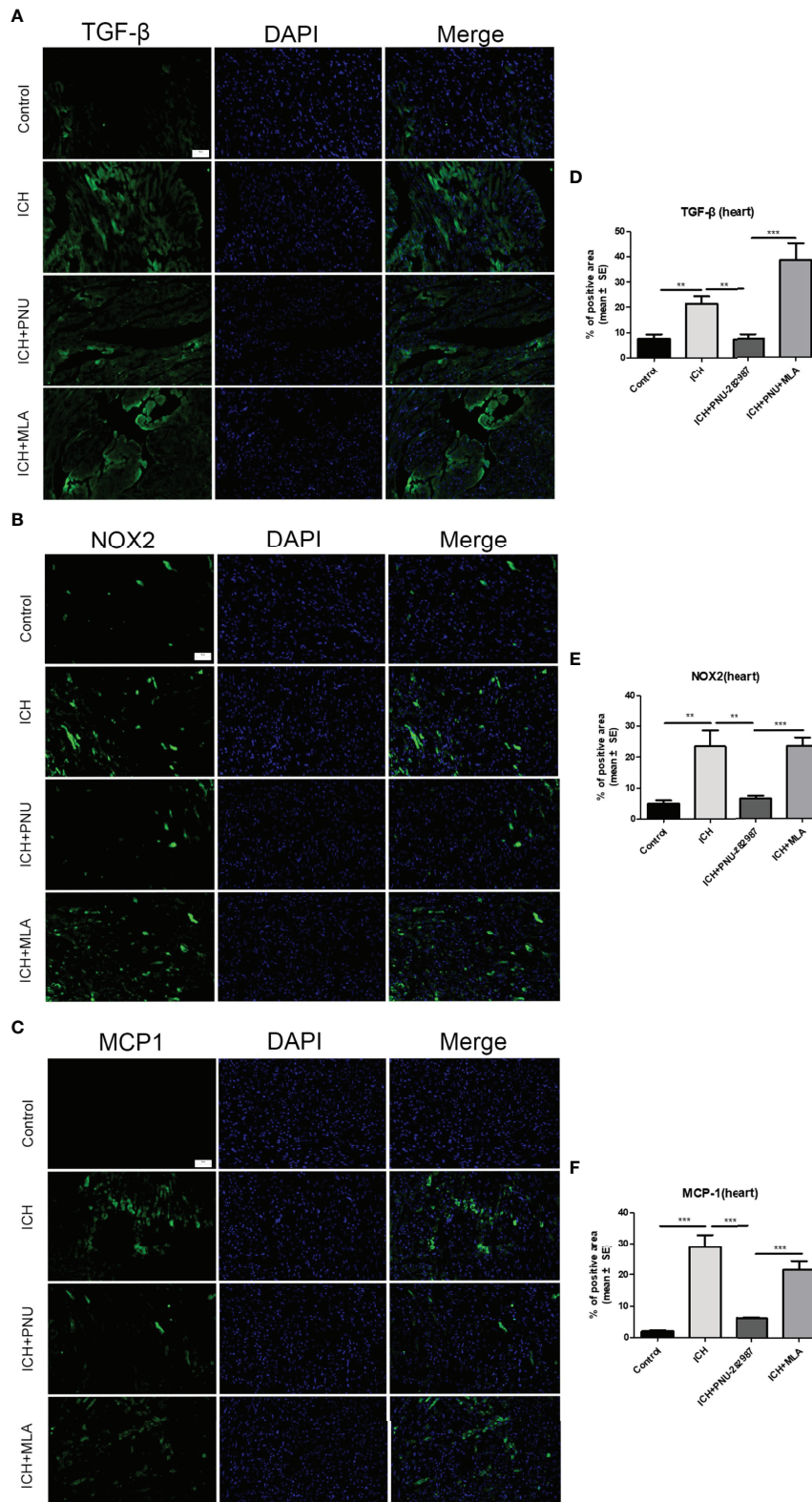


**FIGURE 11** | Activating  $\alpha 7$ nAChR decreased ICH-caused oxidative stress and inflammatory responses in the heart. Immunofluorescence images of inflammation factor of TGF- $\beta$  (A), NOX-2 (B), MCP-1 (C) were compared in four groups in heart. (scale bar, 100  $\mu$ m). Quantitative data of TGF- $\beta$  (D), NOX-2 (E), MCP-1 (F) in heart. n = 6 per group. Data are presented as mean  $\pm$  SE; \*\*P < 0.01; \*\*\*P < 0.0001.

signaling inhibited NF- $\kappa$ B nuclear translocation into macrophages, hence inhibiting the secretion of high mobility group box 1 (HMGB1), an important pro-inflammatory factors and mediator of advanced sepsis (40). Peña et al. demonstrated a new perspective to study the mechanism of cholinergic regulation of inflammation that is attributed to the JAK2/STAT3 signaling cascade. In their study, phosphorylated and unphosphorylated STAT3 were responsible for the anti-inflammatory result (52). Recent researches have also further elucidated alternative mechanisms of cholinergic control of inflammation involving PI3K signaling. Nicotine contributed to an increase in IRAK-M in macrophages *via* a cascade (JAK2/PI3K/STAT3) or both (JAK2/STAT3 and PI3K/STAT3) cascades. The anti-inflammatory effect of  $\alpha 7$ nAChR agonists is due to increased activity of IRAK-M, which has an anti-inflammatory activity (53). Another possible mechanism by which cholinergic modulates pro-inflammatory responses are to increase heme oxygenase 1 (HO-1) activity (53).

In this study, we determined the mechanism of the cholinergic anti-inflammatory pathway in ICH and its role in the therapeutic. We established a collagenase-induced ICH model in mice and determined that the  $\alpha 7$ nAChR agonist PNU-282987 can promote the transformation of macrophages from pro-inflammatory subtype to anti-inflammatory subtype, resulting in inhibition of inflammatory factors to improve neurological and cardiac dysfunction.

Autophagy is a conserved intracellular mechanism that mediated lipid aggregation, degradation of misfolded proteins and damaged organelles. In response to cellular stressors such as starvation and oxidative stress, autophagy is activated to limit cell death. In recent years, the role of autophagy in different neuronal disease models has attracted much attention. As is well known, autophagy is a “double-edged sword”. It was unclear whether autophagy played a beneficial or detrimental role. Some studies demonstrated that impaired autophagic currents are associated with neuronal cell death following TBI (54). Activation of the autophagy pathway *via* an anti-apoptotic mechanism reduced early brain injury in a rat model of SAH (55). Whereas other researchers have shown that autophagy can cause to cell death in focal cerebral ischemia models (56). Furthermore, one study suggested that activation of autophagy pathways played a neuroprotective role in Alzheimer’s disease, which is related to  $\alpha 7$ nAChR signaling (57). The relationship between induction of neuronal autophagy and activation of  $\alpha 7$ nAChR has been proven (58–60). Consistent with these findings, our results indicated that PNU-282987, an  $\alpha 7$ nAChR agonist promoted autophagy, which increased the Beclin, LC3-II/LC3-I ratio and reduced p62/SQSTM1, a marker of autophagic currents activated in ICH model. In our study, activation of  $\alpha 7$ nAChR promoted autophagy, reduced the release of inflammatory factors, and improved brain function and heart function. Administration of 3-MA, which inhibited class III PI3K and comprehensively acted as an autophagy inhibitor, reversed the effect of  $\alpha 7$ nAChR agonist on autophagy after ICH, indicated that the anti-inflammatory effect of  $\alpha 7$ nAChR is related to the

autophagy pathway. However, whether the anti-inflammatory effect caused by promoting autophagy is caused by reducing the death of neurons or cardiomyocytes remains to be determined by further experiments. Whether activation of  $\alpha 7$ nAChR reduced or promoted autophagy remains contentious, as its role is distinct in diverse disease models. A publication has revealed that  $\alpha 7$ nAChR promoted protective autophagy in the LPS-induced mouse acute lung injury model and in MH-S cells (61). Li Z. et al. have also demonstrated that nicotine induced autophagy through the  $\alpha 7$ nAChR-mediated JAK2/STAT3 signaling pathway, thereby promoting the activation of human pancreatic stellate cells (62).

In our research, we found that PNU-282987, a positive allosteric modulator selective for  $\alpha 7$ nAChR, exerted protective effects against ICH damage by modulating the crosstalk between autophagy and inflammation. Although the use of PNU-282987 is limited, this study provides new evidence to support future development of therapeutic strategies for inflammatory diseases such as ICH *via* the cholinergic anti-inflammatory pathway.

## DATA AVAILABILITY STATEMENT

The original contributions presented in the study are included in the article/**Supplementary Material**. Further inquiries can be directed to the corresponding author.

## ETHICS STATEMENT

The animal study was reviewed and approved by the Animal Care and Use Committee of Tianjin Medical University General Hospital.

## AUTHOR CONTRIBUTIONS

TY: experimental design and gave final approval of manuscript. YS: experimental design, wrote the manuscript, performed experiments, analyzed data and prepared figures. WZ: performed experiments, analyzed data, prepared figures. RZ: experimental design and wrote the manuscript. QY, RW, XL, JW, and RL: performed experiments. All authors contributed to the article and approved the submitted version.

## FUNDING

This work was supported by National Natural Science Foundation of China (grant 82171320).

## ACKNOWLEDGMENTS

We thank Helen Robertson, from Liwen Bianji (Edanz) ([www.liwenbianji.cn/](http://www.liwenbianji.cn/)), for editing the English text of a draft of this manuscript.

## REFERENCES

- Qureshi AI, Mendelow AD, Hanley DF. Intracerebral Haemorrhage. *Lancet* (2009) 373(9675):1632–44. doi: 10.1016/s0140-6736(09)60371-8
- Hwang BY, Appelboom G, Ayer A, Kellner CP, Kotchetkov IS, Gigante PR, et al. Advances in Neuroprotective Strategies: Potential Therapies for Intracerebral Hemorrhage. *Cerebrovasc Dis* (2011) 31(3):211–22. doi: 10.1159/000321870
- Chen M, Li X, Zhang X, He X, Lai L, Liu Y, et al. The Inhibitory Effect of Mesenchymal Stem Cell on Blood-Brain Barrier Disruption Following Intracerebral Hemorrhage in Rats: Contribution of Tsg-6. *J Neuroinflamm* (2015) 12:61. doi: 10.1186/s12974-015-0284-x
- Xu C, Wang T, Cheng S, Liu Y. Increased Expression of T Cell Immunoglobulin and Mucin Domain 3 Aggravates Brain Inflammation Via Regulation of the Function of Microglia/Macrophages After Intracerebral Hemorrhage in Mice. *J Neuroinflamm* (2013) 10:141. doi: 10.1186/1742-2094-10-141
- Lei B, Dawson HN, Roulhac-Wilson B, Wang H, Laskowitz DT, James ML. Tumor Necrosis Factor  $\alpha$  Antagonism Improves Neurological Recovery in Murine Intracerebral Hemorrhage. *J Neuroinflamm* (2013) 10:103. doi: 10.1186/1742-2094-10-103
- Zhao Q, Yan T, Li L, Chopp M, Venkat P, Qian Y, et al. Immune Response Mediates Cardiac Dysfunction After Traumatic Brain Injury. *J Neurotrauma* (2019) 36(4):619–29. doi: 10.1089/neu.2018.5766
- Li R, Yuan Q, Su Y, Chopp M, Yan T, Chen J. Immune Response Mediates the Cardiac Damage After Subarachnoid Hemorrhage. *Exp Neurol* (2020) 323:113093. doi: 10.1016/j.expneurol.2019.113093
- Yan T, Chen Z, Chopp M, Venkat P, Zacharek A, Li W, et al. Inflammatory Responses Mediate Brain-Heart Interaction After Ischemic Stroke in Adult Mice. *J Cereb Blood Flow Metab* (2020) 40(6):1213–29. doi: 10.1177/0271678x18813317
- Li W, Li L, Chopp M, Venkat P, Zacharek A, Chen Z, et al. Intracerebral Hemorrhage Induces Cardiac Dysfunction in Mice Without Primary Cardiac Disease. *Front Neurol* (2018) 9:965. doi: 10.3389/fneur.2018.00965
- Kume T, Takada-Takatori Y. Nicotinic Acetylcholine Receptor Signaling: Roles in Neuroprotection. In: A Akaïke, S Shimohama, Y Misu, editors. *Nicotinic Acetylcholine Receptor Signaling in Neuroprotection*. Singapore: Springer Copyright 2018 (2018), p. 59–71.
- Kalashnyk O, Lykhmus O, Oliinyk O, Komisarenko S, Skok M.  $\alpha 7$  Nicotinic Acetylcholine Receptor-Specific Antibody Stimulates Interleukin-6 Production in Human Astrocytes Through P38-Dependent Pathway. *Int Immunopharmacol* (2014) 23(2):475–9. doi: 10.1016/j.intimp.2014.09.022
- Báez-Pagán CA, Delgado-Vélez M, Lasalde-Dominicci JA. Activation of the Macrophage  $\alpha 7$  Nicotinic Acetylcholine Receptor and Control of Inflammation. *J Neuroimmune Pharmacol* (2015) 10(3):468–76. doi: 10.1007/s11481-015-9601-5
- Egea J, Buendia I, Parada E, Navarro E, León R, Lopez MG. Anti-Inflammatory Role of Microglial Alpha7 Nachrs and Its Role in Neuroprotection. *Biochem Pharmacol* (2015) 97(4):463–72. doi: 10.1016/j.bcp.2015.07.032
- Han B, Li X, Hao J. The Cholinergic Anti-Inflammatory Pathway: An Innovative Treatment Strategy for Neurological Diseases. *Neurosci Biobehav Rev* (2017) 77:358–68. doi: 10.1016/j.neubiorev.2017.04.002
- Krafft PR, Altay O, Rolland WB, Duris K, Lekic T, Tang J, et al.  $\alpha 7$  Nicotinic Acetylcholine Receptor Agonism Confers Neuroprotection Through Gsk-3 $\beta$  Inhibition in a Mouse Model of Intracerebral Hemorrhage. *Stroke* (2012) 43(3):844–50. doi: 10.1161/strokeaha.111.639989
- Hijioka M, Matsushita H, Ishibashi H, Hisatsune A, Isohama Y, Katsuki H.  $\alpha 7$  Nicotinic Acetylcholine Receptor Agonist Attenuates Neuropathological Changes Associated With Intracerebral Hemorrhage in Mice. *Neuroscience* (2012) 222:10–9. doi: 10.1016/j.neuroscience.2012.07.024
- Rubinsztein DC, Bento CF, Deretic V. Therapeutic Targeting of Autophagy in Neurodegenerative and Infectious Diseases. *J Exp Med* (2015) 212(7):979–90. doi: 10.1084/jem.20150956
- Ke P, Shao BZ, Xu ZQ, Chen XW, Liu C. Intestinal Autophagy and Its Pharmacological Control in Inflammatory Bowel Disease. *Front Immunol* (2016) 7:695. doi: 10.3389/fimmu.2016.00695
- Shao BZ, Han BZ, Zeng YX, Su DF, Liu C. The Roles of Macrophage Autophagy in Atherosclerosis. *Acta Pharmacol Sin* (2016) 37(2):150–6. doi: 10.1038/aps.2015.87
- Bravo-San Pedro JM, Kroemer G, Galluzzi L. Autophagy and Mitophagy in Cardiovascular Disease. *Circ Res* (2017) 120(11):1812–24. doi: 10.1161/circresaha.117.311082
- van Asch CJ, Luitse MJ, Rinkel GJ, van der Tweel I, Algra A, Klijn CJ. Incidence, Case Fatality, and Functional Outcome of Intracerebral Haemorrhage Over Time, According to Age, Sex, and Ethnic Origin: A Systematic Review and Meta-Analysis. *Lancet Neurol* (2010) 9(2):167–76. doi: 10.1016/s1474-4422(09)70340-0
- Wang LF, Yokoyama KK, Chen TY, Hsiao HW, Chiang PC, Hsieh YC, et al. Male-Specific Alleviation of Iron-Induced Striatal Injury by Inhibition of Autophagy. *PLoS One* (2015) 10(7):e0131224. doi: 10.1371/journal.pone.0131224
- Shao BZ, Ke P, Xu ZQ, Wei W, Cheng MH, Han BZ, et al. Autophagy Plays an Important Role in Anti-Inflammatory Mechanisms Stimulated by Alpha7 Nicotinic Acetylcholine Receptor. *Front Immunol* (2017) 8:553. doi: 10.3389/fimmu.2017.00553
- Shao BZ, Wang SL, Fang J, Li ZS, Bai Y, Wu K. Alpha7 Nicotinic Acetylcholine Receptor Alleviates Inflammatory Bowel Disease Through Induction of Ampk-Mtor-P70s6k-Mediated Autophagy. *Inflammation* (2019) 42(5):1666–79. doi: 10.1007/s10753-019-01027-9
- Chang KW, Zong HF, Ma KG, Zhai WY, Yang WN, Hu XD, et al. Activation of  $\alpha 7$  Nicotinic Acetylcholine Receptor Alleviates A $\beta$ (1-42)-Induced Neurotoxicity Via Downregulation of P38 and Jnk Mapk Signaling Pathways. *Neurochem Int* (2018) 120:238–50. doi: 10.1016/j.neuint.2018.09.005
- Shao Z, Li Q, Wang S, Chen Z. Protective Effects of PNU-282987 on Sepsis-Induced Acute Lung Injury in Mice. *Mol Med Rep* (2019) 19(5):3791–8. doi: 10.3892/mmr.2019.10016
- Li F, Chen Z, Pan Q, Fu S, Lin F, Ren H, et al. The Protective Effect of PNU-282987, a Selective  $\alpha 7$  Nicotinic Acetylcholine Receptor Agonist, on the Hepatic Ischemia-Reperfusion Injury Is Associated With the Inhibition of High-Mobility Group Box 1 Protein Expression and Nuclear Factor  $\kappa$ b Activation in Mice. *Shock* (2013) 39(2):197–203. doi: 10.1097/SHK.0b013e31827aa1f6
- Li YF, LaCroix C, Freeling J. Specific Subtypes of Nicotinic Cholinergic Receptors Involved in Sympathetic and Parasympathetic Cardiovascular Responses. *Neurosci Lett* (2009) 462(1):20–3. doi: 10.1016/j.neulet.2009.06.081
- Li YF, Lacroix C, Freeling J. Cytisine Induces Autonomic Cardiovascular Responses Via Activations of Different Nicotinic Receptors. *Auton Neurosci* (2010) 154(1-2):14–9. doi: 10.1016/j.autneu.2009.09.023
- Callahan PM, Hutchings EJ, Kille NJ, Chapman JM, Terry AV Jr. Positive Allosteric Modulator of  $\alpha 7$  Nicotinic-Acetylcholine Receptors, Pnu-120596 Augments the Effects of Donepezil on Learning and Memory in Aged Rodents and Non-Human Primates. *Neuropharmacology* (2013) 67:201–12. doi: 10.1016/j.neuropharm.2012.10.019
- MacLellan CL, Silasi G, Poon CC, Edmundson CL, Buist R, Peeling J, et al. Intracerebral Hemorrhage Models in Rat: Comparing Collagenase to Blood Infusion. *J Cereb Blood Flow Metab* (2008) 28(3):516–25. doi: 10.1038/sj.jcbfm.9600548
- Khalil H, Kanisicak O, Prasad V, Correll RN, Fu X, Schips T, et al. Fibroblast-Specific Tgf- $\beta$ -Smad2/3 Signaling Underlies Cardiac Fibrosis. *J Clin Invest* (2017) 127(10):3770–83. doi: 10.1172/jci94753

## SUPPLEMENTARY MATERIAL

The Supplementary Material for this article can be found online at: <https://www.frontiersin.org/articles/10.3389/fimmu.2022.870174/full#supplementary-material>

33. Ma Y, Kuang Y, Bo W, Liang Q, Zhu W, Cai M, et al. Exercise Training Alleviates Cardiac Fibrosis Through Increasing Fibroblast Growth Factor 21 and Regulating Tgf- $\beta$ 1-Smad2/3-Mmp2/9 Signaling in Mice With Myocardial Infarction. *Int J Mol Sci* (2021) 22(22):12341. doi: 10.3390/ijms222212341
34. Medeiros NI, Gomes JAS, Fiuza JA, Sousa GR, Almeida EF, Novaes RO, et al. MMP-2 and MMP-9 Plasma Levels Are Potential Biomarkers for Indeterminate and Cardiac Clinical Forms Progression in Chronic Chagas Disease. *Sci Rep* (2019) 9(1):14170. doi: 10.1038/s41598-019-50791-z
35. Li H, Wu J, Shen H, Yao X, Liu C, Pianta S, et al. Autophagy in Hemorrhagic Stroke: Mechanisms and Clinical Implications. *Prog Neurobiol* (2018) 163-164:79–97. doi: 10.1016/j.pneurobio.2017.04.002
36. Wang Y, Smith W, Hao D, He B, Kong L. M1 and M2 Macrophage Polarization and Potentially Therapeutic Naturally Occurring Compounds. *Int Immunopharmacol* (2019) 70:459–66. doi: 10.1016/j.intimp.2019.02.050
37. Murray PJ. Macrophage Polarization. *Annu Rev Physiol* (2017) 79:541–66. doi: 10.1146/annurev-physiol-022516-034339
38. Li XW, Wang H. Non-Neuronal Nicotinic Alpha 7 Receptor, a New Endothelial Target for Revascularization. *Life Sci* (2006) 78(16):1863–70. doi: 10.1016/j.lfs.2005.08.031
39. Liu C, Su D. Nicotinic Acetylcholine Receptor  $\alpha 7$  Subunit: A Novel Therapeutic Target for Cardiovascular Diseases. *Front Med* (2012) 6(1):35–40. doi: 10.1007/s11684-012-0171-0
40. Wang H, Liao H, Ochani M, Justiniani M, Lin X, Yang L, et al. Cholinergic Agonists Inhibit Hmgb1 Release and Improve Survival in Experimental Sepsis. *Nat Med* (2004) 10(11):1216–21. doi: 10.1038/nm1124
41. Su X, Lee JW, Matthay ZA, Mednick G, Uchida T, Fang X, et al. Activation of the Alpha7 NACHR Reduces Acid-Induced Acute Lung Injury in Mice and Rats. *Am J Respir Cell Mol Biol* (2007) 37(2):186–92. doi: 10.1165/rcmb.2006-0240OC
42. Zhang Q, Lu Y, Bian H, Guo L, Zhu H. Activation of the  $\alpha 7$  Nicotinic Receptor Promotes Lipopolysaccharide-Induced Conversion of M1 Microglia to M2. *Am J Transl Res* (2017) 9(3):971–85.
43. Hao J, Simard AR, Turner GH, Wu J, Whiteaker P, Lukas RJ, et al. Attenuation of CNS Inflammatory Responses by Nicotine Involves  $\alpha 7$  and Non- $\alpha 7$  Nicotinic Receptors. *Exp Neurol* (2011) 227(1):110–9. doi: 10.1016/j.expneurol.2010.09.020
44. Nizri E, Irony-Tur-Sinai M, Lory O, Orr-Urtreger A, Lavi E, Brenner T. Activation of the Cholinergic Anti-Inflammatory System by Nicotine Attenuates Neuroinflammation Via Suppression of Th1 and Th17 Responses. *J Immunol* (2009) 183(10):6681–8. doi: 10.4049/jimmunol.0902212
45. Nizri E, Irony-Tur-Sinai M, Faranesh N, Lavon I, Lavi E, Weinstock M, et al. Suppression of Neuroinflammation and Immunomodulation by the Acetylcholinesterase Inhibitor Rivastigmine. *J Neuroimmunol* (2008) 203(1):12–22. doi: 10.1016/j.jneuroim.2008.06.018
46. Han Z, Shen F, He Y, Degos V, Camus M, Maze M, et al. Activation of  $\alpha 7$  Nicotinic Acetylcholine Receptor Reduces Ischemic Stroke Injury Through Reduction of Pro-Inflammatory Macrophages and Oxidative Stress. *PLoS One* (2014) 9(8):e105711. doi: 10.1371/journal.pone.0105711
47. Krafft PR, McBride D, Rolland WB, Lekic T, Flores JJ, Zhang JH.  $\alpha 7$  Nicotinic Acetylcholine Receptor Stimulation Attenuates Neuroinflammation Through Jak2-Stat3 Activation in Murine Models of Intracerebral Hemorrhage. *BioMed Res Int* (2017) 2017:8134653. doi: 10.1155/2017/8134653
48. Jiang T, Wu M, Zhang Z, Yan C, Ma Z, He S, et al. Electroacupuncture Attenuated Cerebral Ischemic Injury and Neuroinflammation Through  $\alpha 7$ nAChR-Mediated Inhibition of NLRP3 Inflammasome in Stroke Rats. *Mol Med* (2019) 25(1):22. doi: 10.1186/s10020-019-0091-4
49. Nishio T, Taura K, Iwasako K, Koyama Y, Tanabe K, Yamamoto G, et al. Hepatic Vagus Nerve Regulates Kupffer Cell Activation Via  $\alpha 7$  Nicotinic Acetylcholine Receptor in Nonalcoholic Steatohepatitis. *J Gastroenterol* (2017) 52(8):965–76. doi: 10.1007/s00535-016-1304-z
50. Teng P, Liu Y, Dai Y, Zhang H, Liu WT, Hu J. Nicotine Attenuates Osteoarthritis Pain and Matrix Metalloproteinase-9 Expression Via the  $\alpha 7$  Nicotinic Acetylcholine Receptor. *J Immunol* (2019) 203(2):485–92. doi: 10.4049/jimmunol.1801513
51. Sundman E, Olofsson PS. Neural Control of the Immune System. *Adv Physiol Educ* (2014) 38(2):135–9. doi: 10.1152/advan.00094.2013
52. Peña G, Cai B, Liu J, van der Zanden EP, Deitch EA, de Jonge WJ, et al. Unphosphorylated Stat3 Modulates Alpha 7 Nicotinic Receptor Signaling and Cytokine Production in Sepsis. *Eur J Immunol* (2010) 40(9):2580–9. doi: 10.1002/eji.201040540
53. Maldifassi MC, Atienza G, Arnalich F, López-Collazo E, Cedillo JL, Martín-Sánchez C, et al. A New Irak-M-Mediated Mechanism Implicated in the Anti-Inflammatory Effect of Nicotine Via  $\alpha 7$  Nicotinic Receptors in Human Macrophages. *PLoS One* (2014) 9(9):e108397. doi: 10.1371/journal.pone.0108397
54. Sarkar C, Zhao Z, Aungst S, Sabirzhanov B, Faden AI, Lipinski MM. Impaired Autophagy Flux Is Associated With Neuronal Cell Death After Traumatic Brain Injury. *Autophagy* (2014) 10(12):2208–22. doi: 10.4161/15548627.2014.981787
55. Jing CH, Wang L, Liu PP, Wu C, Ruan D, Chen G. Autophagy Activation Is Associated With Neuroprotection Against Apoptosis Via a Mitochondrial Pathway in a Rat Model of Subarachnoid Hemorrhage. *Neuroscience* (2012) 213:144–53. doi: 10.1016/j.neuroscience.2012.03.055
56. Rami A, Langhagen A, Steiger S. Focal Cerebral Ischemia Induces Upregulation of Beclin 1 and Autophagy-Like Cell Death. *Neurobiol Dis* (2008) 29(1):132–41. doi: 10.1016/j.nbd.2007.08.005
57. Hung SY, Huang WP, Liou HC, Fu WM. Autophagy Protects Neuron From Abeta-Induced Cytotoxicity. *Autophagy* (2009) 5(4):502–10. doi: 10.4161/auto.5.4.8096
58. Nakamura S, Oba M, Suzuki M, Takahashi A, Yamamuro T, Fujiwara M, et al. Suppression of Autophagic Activity by Rubicon Is a Signature of Aging. *Nat Commun* (2019) 10(1):847. doi: 10.1038/s41467-019-08729-6
59. Mizushima N, Yoshimori T, Levine B. Methods in Mammalian Autophagy Research. *Cell* (2010) 140(3):313–26. doi: 10.1016/j.cell.2010.01.028
60. Dudek J, Hartmann M, Rehling P. The Role of Mitochondrial Cardiolipin in Heart Function and Its Implication in Cardiac Disease. *Biochim Biophys Acta Mol Basis Dis* (2019) 1865(4):810–21. doi: 10.1016/j.bbdis.2018.08.025
61. Zhao X, Yu Z, Lv Z, Meng L, Xu J, Yuan S, et al. Activation of Alpha-7 Nicotinic Acetylcholine Receptors ( $\alpha 7$ nAChR) Promotes the Protective Autophagy in Lps-Induced Acute Lung Injury (Ali) in Vitro and in Vivo. *Inflammation* (2019) 42(6):2236–45. doi: 10.1007/s10753-019-01088-w
62. Li Z, Zhang X, Jin T, Hao J. Nicotine Promotes Activation of Human Pancreatic Stellate Cells Through Inducing Autophagy Via  $\alpha 7$ nAChR-Mediated Jak2/Stat3 Signaling Pathway. *Life Sci* (2020) 243:117301. doi: 10.1016/j.lfs.2020.117301

**Conflict of Interest:** The authors declare that the research was conducted in the absence of any commercial or financial relationships that could be construed as a potential conflict of interest.

**Publisher's Note:** All claims expressed in this article are solely those of the authors and do not necessarily represent those of their affiliated organizations, or those of the publisher, the editors and the reviewers. Any product that may be evaluated in this article, or claim that may be made by its manufacturer, is not guaranteed or endorsed by the publisher.

Copyright © 2022 Su, Zhang, Zhang, Yuan, Wu, Liu, Wuri, Li and Yan. This is an open-access article distributed under the terms of the Creative Commons Attribution License (CC BY). The use, distribution or reproduction in other forums is permitted, provided the original author(s) and the copyright owner(s) are credited and that the original publication in this journal is cited, in accordance with accepted academic practice. No use, distribution or reproduction is permitted which does not comply with these terms.